THE REVIEW OF PHYSICAL CHEMISTRY OF JAPAN, VOL. 40, NO. 2, 1970

PRESSURE EFFECTS ON SOLID STATE POLYMERIC TRANSFORMATIONS*

BY JIRO OSUGI

Under the title of "Behavior of Polymeric Solid under Pressure", I wish to mention on physical and chemical transformations of polymeric solids under pressure.

On the physical transformation, we studied on the crystallization and the melting of polyethylene under pressures up to 30 kb.

The single crystal mat of polyethylene (Marlex 50) suspended in silicone oil was aged isothermally at a fixed temperature and pressure for 3 hours. The thickening process of the sample was examined by small angle X-ray diffraction measurements. Fig. 1 shows the long period of chain folding against annealing temperature at various pressures. Thickness of the single crystal lamella can be well expressed by the equation of Lauritzen-Hoffman up to 2 kb, as shown in Fig. 2. From the following equation,

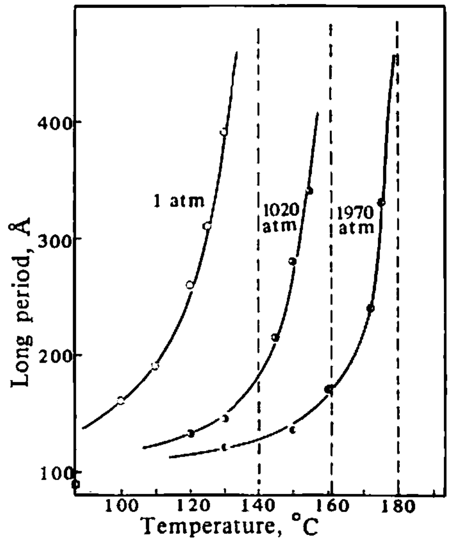

Fig. 1 Thickness of single crystal at various pressure and temperature

---

(*Received November 15, 1970*)

* Lecture invited at the First Joint CWRU-MIT Polymer Symposium, in Cambridge, Mass., U. S. A., on October 27, 1970

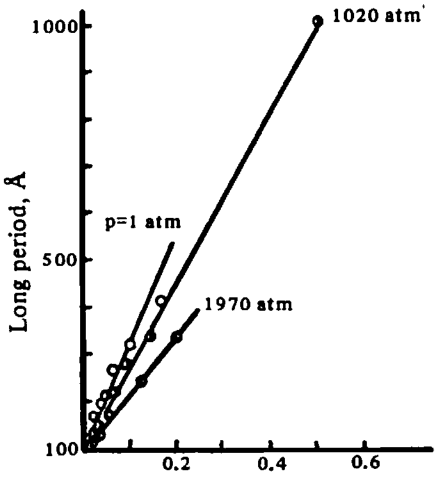

Fig. 2 Plot of L against $1/(T_m\text{-}T)$ for Marlex 50 crystallized at various pressures

$$L = \frac{kT}{d_0\sigma_s} + \frac{2\sigma_e}{f_u}\,, \qquad f_u = \Delta h(T_m - T)/T_m$$

$$L = L_0 + \frac{A}{T_m - T}\,, \qquad A = \frac{2\sigma_e T_m}{\Delta h}$$

we obtained the melting point, which is the asymptotes of each curve in Fig. 1. These values well coincided with other values of extended polymer, as shown in Fig. 3 cited from the literatures.

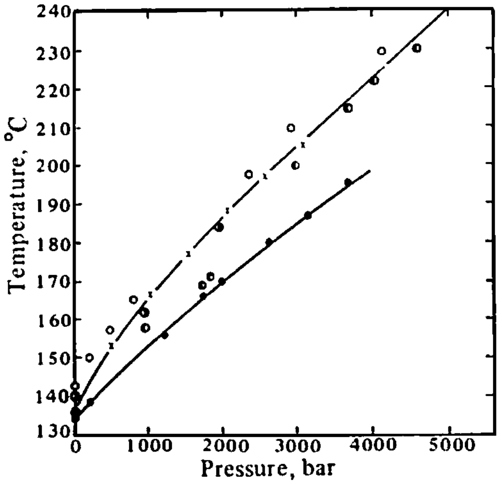

Fig. 3 Melting temperature versus pressure: (○) Davidson and Wunderlich, DTA data on extended chain crystals; (×) Baer and Kardos, dilatometry data; (●) Davidson and Wunderlich, DTA data on folded chain crystals: (◑), (◐) Osugi, *et al.*

We can conclude the effects of pressure are chiefly dependent on the elevation of the melting point, but A in the above equation is dependent on pressure, as seen in Fig. 2.

The experimental results where the T-P curve of melting points, as shown in Fig. 4, was crossed, from melt to crystal, by the elevation of pressure up to 2 kb at a fixed temperature of 180°C showed no essential pressure effects on their folding behavior of single crystals and bulk pellets of polyethylene, examined by X-ray and differential scanning calorimeter (DSC). They showed no special orientation and low melting point, respectively.

The melting point of polyethylene was determined by a high pressure apparatus of the piston-cylinder (to 5 kb) where the volume changes were measured, and by an apparatus of cubic anvil (to 30 kb) where the DTA method was used. The results are shown in Fig. 4. As it was shown previously in Fig. 3, the values obtained up to 5 kb were in the range between that of folded chain and extended chain. The melting points were well predicted from Clapeyron's equation up to 5 kb. The volume change ΔV measured, the enthalpy change ΔH and the entropy change ΔS of the melting are shown in Figs. 5, 6 and 7, respectively. It is remarkable that these changes of thermodynamic

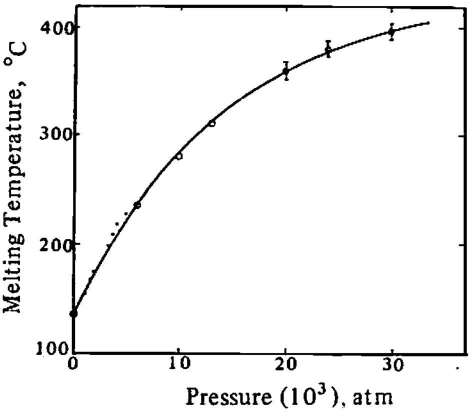

Fig. 4 Melting curve of polyethylene up to 30,000 atm

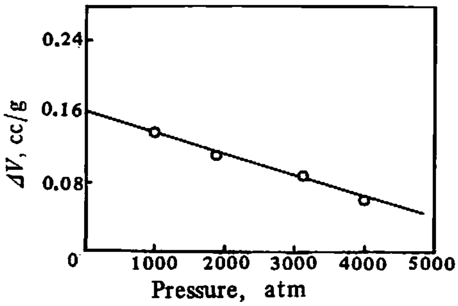

Fig. 5 Variation of ΔV with pressure

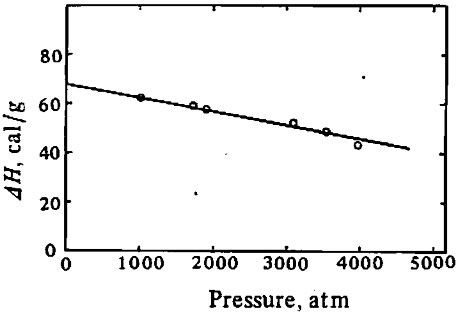

Fig. 6 Variation of ΔH with pressure

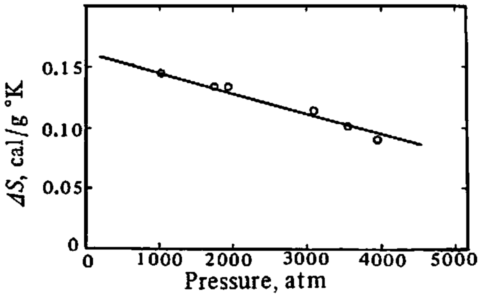

Fig. 7 Variation of ΔS with pressure

properties are almost linearly decreased with the increase of pressure. It may be interesting that ΔS, which is mainly due to configurational entropy, comes to nearly zero around the pressure of 10 kb. This means that liquid may have the solid-like orientation.

Next, the single crystal mat and bulk pellet compressed by the cubic anvil apparatus up to 25 kb at a fixed temperature of 350°C for 30 minutes showed the following results. On the single crystal mat, the X-ray diffraction pattern shows a macroscopic orientation (*b*-axis) of the chain molecules as shown in Fig. 8 and the DSC measurements shows the melting curve characteristic to the extended chain crystals, as shown in Fig. 9. It has a small shoulder and a small peak of unstable crystals. On the bulk pellet, the X-ray diffraction pattern shows the different type orientation (*a*-axis) of molecular chain, as shown in Fig. 10 and the DSC measurements shows a peak characteristic to the extended chain crystals, as shown in Fig. 11.

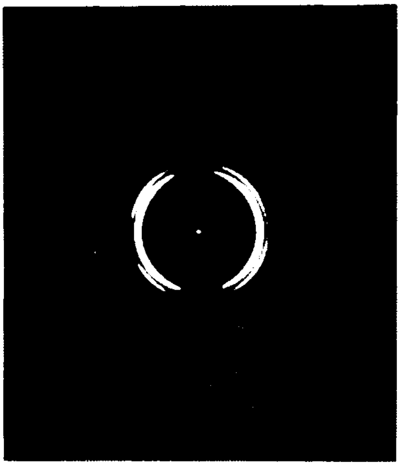

Fig. 8 X-ray diagram of PE crystallized from the melt by the pressure elevation at fixed temp. (350°C, 15kb→25kb) Original sample is the single crystals mats

For the consideration of these facts, I will discuss high pressure system. Even in gaseous state,

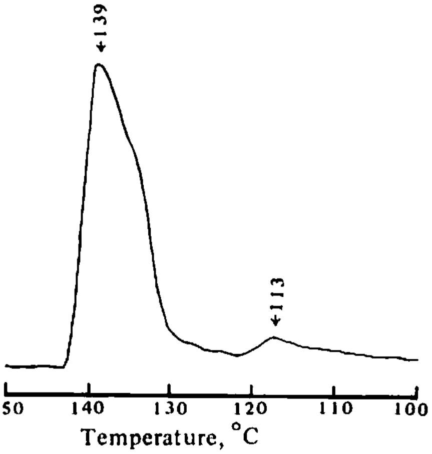

Fig. 9 DSC diagram of PE crystallized from the melt by the pressure elevation at fixed temp. (350°C, 15kb→25kb) Original sample is the single crystals mats

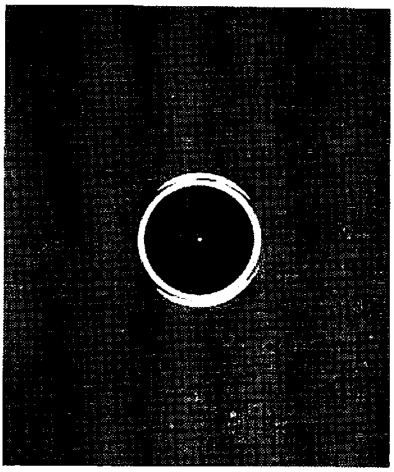

Fig. 10 X-ray diagram of PE crystallized from the melt by the pressure elevation at fixed temp. (350°C, 15kb→25kb) Original sample is the bulk pellets.

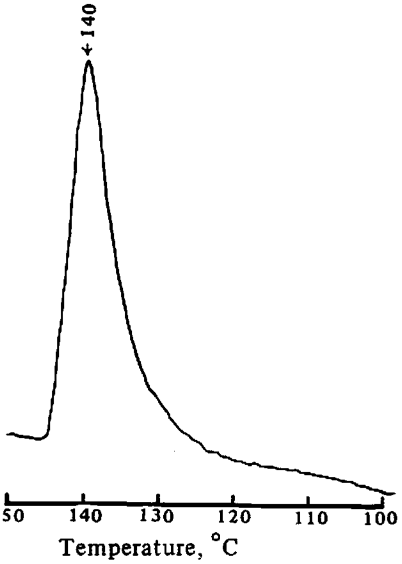

Fig. 11 DSC diagram of PE crystallized from the melt by the pressure elevation at fixed temp. (350°C. 15kb→25kb) Original sample is the bulk pellets.

the potential between molecules is repulsive and molecules are deformed and orientated at the higher pressure than 10 kb. Fig. 12 shows PV against P diagram of nitrogen. The curve is not horizontal and not linear but is concaved downward. This is expressed by the equation,

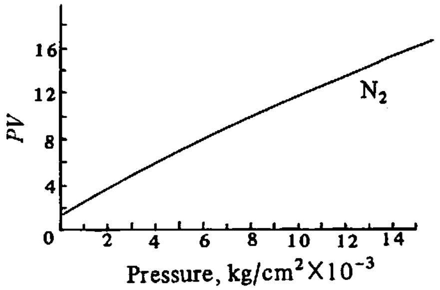

Fig. 12

$$PV = c + aP - bP^2,$$
$$P[V - (a - bP)] = C.$$

This means that molecules are compressible and deformable.

In the following equation of thermodynamics,

$$\left(\frac{\partial E}{\partial P}\right)_T = -T\left(\frac{\partial V}{\partial T}\right)_P - P\left(\frac{\partial V}{\partial P}\right)_T,$$

the first term in the right hand side of the equation is dominant and shows attractive molecular force at lower pressure, but at the pressure range higher than 10 kb, the second is dominant. This means that molecules in this higher range of pressure are repulsive each other, and are deformed and orientated. It may be true that the orientation of deformed molecules is existent in the melt of chain molecule, as suggested from X-ray diffraction pattern of Figs. 8 and 10.

At a pressure of 25 kb, we found the orientation of molecular chain and the rapid rate of chain extending crystallization. This may be the case in trans-zigzag conformation of polyethylene chain molecule. On the other hand, we compressed the polypropylene up to 35 kb and 370°C. In contrast to these results, the extention of polymer chain of polypropylene was not observed and the acceleration of crystallization by pressure could not be confirmed. However, in this case, we found the change of crystalline modifications. These facts might be due to the helical conformation of polymer chain of polypropylene.

In addition, the sample repeatedly compressed and decompressed by the piston-cylinder apparatus up to 5 kb at a temperature of 230°C shows the pictures of electron microscope as shown in the next three pictures 13, 14 and 15. They have figures of extended chains crystals (the black image is due to the adhesion of the original sample). But by X-ray, no orientation effect is observed. The DSC

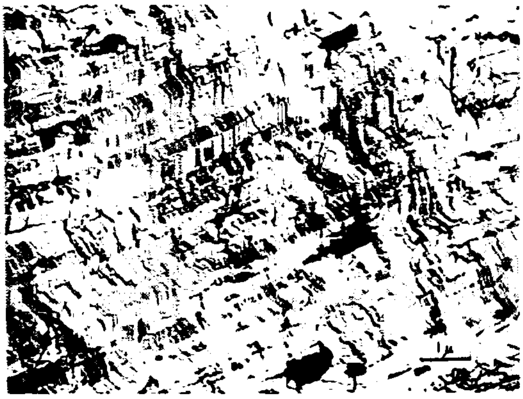

Fig. 13 Fracture surface of polyethylene sample crystallized at 230°C under 5000 atm

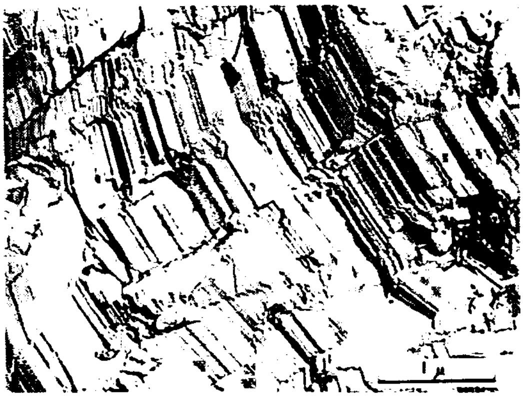

Fig. 14 Fracture surface of polyethylene sample crystallized at 230°C under 5000 atm

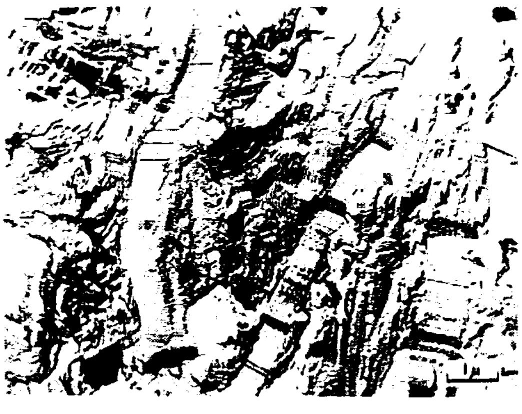

Fig. 15 Fracture surface of polyethylene sample crystallized at 230°C under 5000 atm

diagram of the sample shows three peaks at the end of the sample rod (Fig. 16) and the two peaks at the center of the rod (Fig. 17). The highest peak at 142°C is characteristic to the melting of extended chain crystals. They have other low peaks of folded chain crystals. The end of the tail of the curve is 145°C.

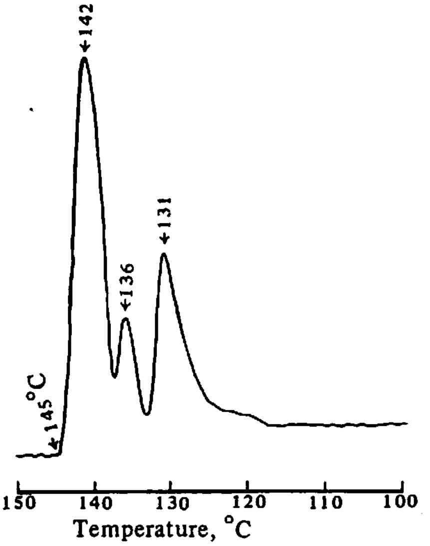

Fig. 16 DSC diagram of PE crystallized from the melt by the pressure elevation at fixed temp. (230°C, 5kb)
Original sample is the bulk pellets.

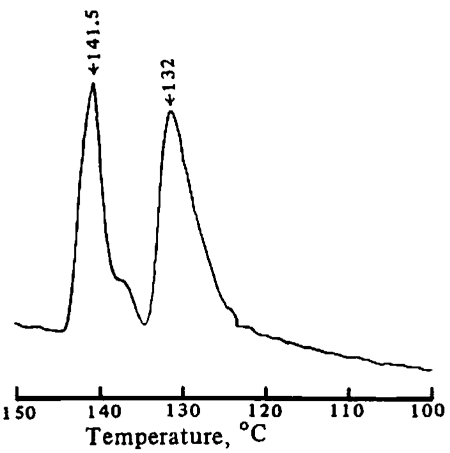

Fig. 17 DSC diagram of PE crystallized from the melt by the pressure elevation at fixed temp. (230°C, 5kb)
Original samgle is the bulk pellets.

On the chemical transformations, we studied solid state polymerization reactions under the pressures up to 50 kb.

In advance of the discussions on solid reactions, I wish to mention the freezing polymerization

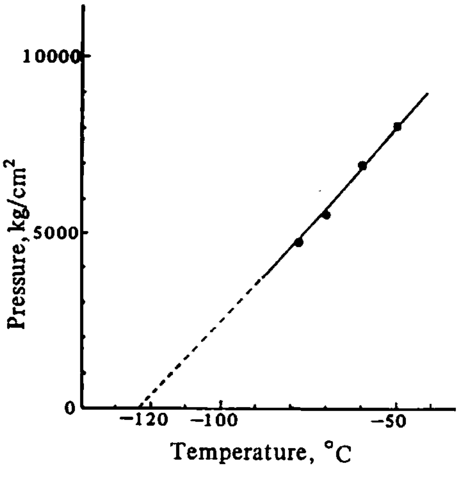

Fig. 18 The limiting pressure for the polymerization

of acetaldehyde at the high pressures up to 10 kb. We found the limiting pressure of polymerization coincided exactly with the transition pressure from liquid to solid in the pressure range of 4 kb to 9 kb, as shown in Fig. 18 (the temperature range from −78°C to −50°C). From the initial rate, we obtained the activation heat and the activation entropy. Further consideration shows that the nucleus for crystallization acts as an initiator of the polymerization and the activation entropy plays a dominant role, as the high pressure effects on polymerization as you know. The thermodynamic relation,

$$\left(\frac{\partial \Delta S^{\ddagger}}{\partial P}\right)_T = -\left(\frac{\partial \Delta V^{\ddagger}}{\partial T}\right)_P ,$$

is held in this reaction, as shown in Table 1. $(\partial \Delta V^{\ddagger}/\partial T)$ is negative and usually $\left(\frac{\partial V}{\partial T}\right)_P > 0$,

Table 1

Pressure (kg/cm^2)	5625	6190	6750	7310	7875	8440
$\Delta S^{\ddagger}$ (cal/mole·deg)	−97.2	−95.3	−93.1	−92.1	−90.0	−88.6

$\Delta\Delta S^{\ddagger}/\Delta P = 0.20$ml/deg·mole

Temperature (°C)	−78	−70	−60
$\Delta V^{\ddagger}$ (ml/mole)	−6.2	−8.0	−11.1

$\Delta\Delta V^{\ddagger}/\Delta T = -0.26$ml/deg·mole

this means that the change in volume occurs chiefly in the initial state ($\Delta V^{\ddagger} = V_{\text{transition}} - V_{\text{initial}}$), so the change in entropy occurs in the initial state. This means that the monomers in the initial state should be arranged to be favorable orientation to polymerize. The similarity of the orientated structure of monomer to the structure of polymer, as supposed from the crystalline structure, is very important.

The topo-chemical access of reacting site of the reactants is the necessary condition for the solid state reaction as shown in Table 2. This table shows the critical distance for reactions is about 4 Å.

The crystalline solid under the pressure higher than 10 kb is in the repulsive potential field, deformed and is closely orientated as mentioned above. This effect of pressure reduces or eliminates

Table 2

Packing type	Doube bond separation	Photo-product	
α	3.6~4.1 Å	α-Truxillic acid	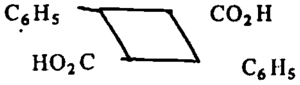
β	3.9~4.1 Å	β-Truxillic acid	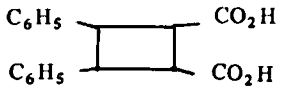
γ	4.7~5.1 Å	No reaction	

the topo-chemical control. And the shrinkage of bond distances by polymerization is compensated by the release of distance in the repulsive field. And the sterically hindered reaction may occur under high pressure as shown in the polymerization of tetramethyl ethylene under the pressure of 35 kb and in other examples. And, further, the high pressure retards the melting and decomposition as already shown in the melting curve of polyethylene up to 30 kb. The stress due to applying pressure may produce dislocation as the initiator of polymerization. So we will find the wide and interesting field of chemical solid reaction under the pressure higher than 10 kb.

As an example, we studied the polymerization of trioxane, that is, cyclic trimer of formaldehyde. This reaction occurred in solid state without catalyst by applying the pressure of 15 kb. as shown Fig. 19. The access of the reacting sites is possible. because the well orientated monomer comes nearer by the pressure.

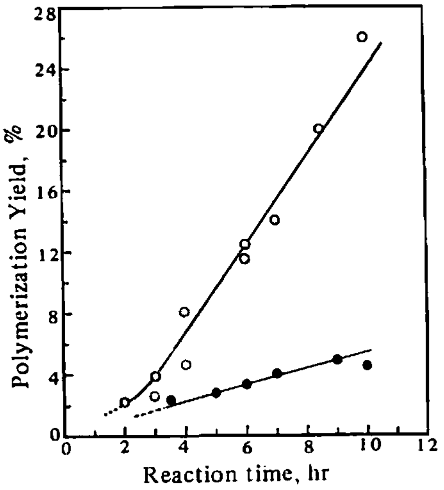

Fig. 19 Polymerization yield-time curves at 15,000 kg/cm^2
○: 120 °C ●: 80 °C

Table 3

Crystarographic Data for Compound

Polymerizable in Solid State

Compound	Formula	Intermolecular contacts	Radiation
Acetaldehyde	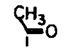	$C_{(1)} \cdots O$ 3.15	γ
Acrylic acid	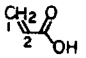	$C_{(1)} \cdots C_{(1)}$ 3.53 3.66 $C_{(2)} \cdots C_{(2)}$ 3.82 $C_{(1)} \cdots C_{(2)}$ 4.05	γ UV
5-Bromo-2-metoxy-cis-cinnamic acid	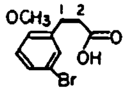	$C_{(1)} \cdots C_{(2)}$ 3.9 $C_{(1)} \cdots C_{(1)}$ 4.0 $C_{(2)} \cdots C_{(2)}$ 4.0	UV
Cyanuric chloride	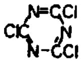	$C \cdots N$ 4.0	γ
Diacetylene dicarboxylic acid	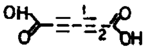	$C_{(1)} \cdots C_{(1)}$ 3.75 $C_{(2)} \cdots C_{(2)}$ 3.75	X, UV
Diketene	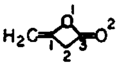	$C_{(2)} \cdots C_{(3)}$ 3.73 $C_{(3)} \cdots C_{(1)}$ 3.75 $C_{(1)} \cdots C_{(2)}$ 3.44	γ
Methyl-m-bromo-trans-cinnamate	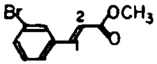	$C_{(1)} \cdots C_{(2)}$ 3.53	UV
Phosphonitrilic chloride trimer	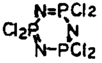	$P \cdots N$ 3.95	X
Thiophene acrylic acid	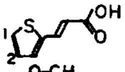	$C_{(1)} \cdots C_{(2)}$ 3.80	UV
Trioxane	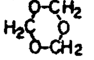	$C \cdots O$ 3.7	γ

Not Polymerizable in Solid State

Compound	Formula	Intermolecular contacts	Radiation
Diphenyl diacetylene	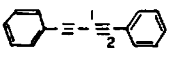	$C_{(2)} \cdots C_{(2)}$ 4.71 $C_{(1)} \cdots C_{(2)}$ 4.87	
Maleic anhydride		$C_{(1)} \cdots C_{(1)}$ 4.28 4.59	
Stilbene	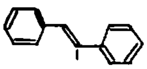	$C_{(1)} \cdots C_{(1)}$ 4.66 4.95	
Tolane	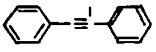	$C_{(1)} \cdots C_{(1)}$ 5.55 5.73	

Further works on solid reactions is mentioned on the polymerization of dinitriles; malononirile and succinonitrile, and polyacrylonitrile. These polymerization reactions were followed by the infrared absorption measurements where the absorption peak (2,247 cm^{-1}) of —C≡N stretching decreased and the peak (1,650~1,550 cm^{-1}) of $(\text{-C=N-})_n$ absorption increased. This shows that the main reaction is

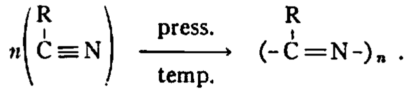

$$n\left(\overset{\overset{\displaystyle R}{|}}{C}\equiv N\right) \xrightarrow[\text{temp.}]{\text{press.}} (\text{-}\overset{\overset{\displaystyle R}{|}}{C}=N\text{-})_n\ .$$

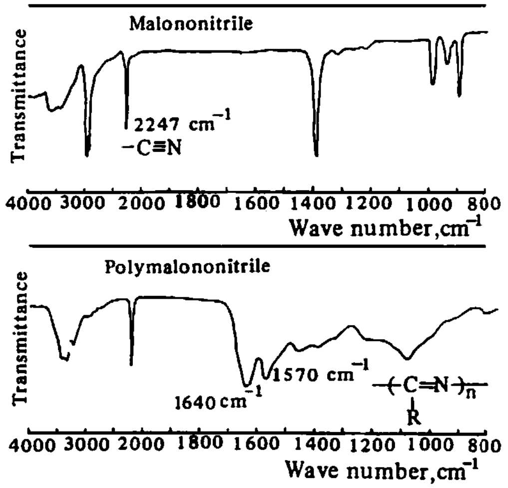

Fig. 20

And the electric conductivity measurement showed that the products were semiconductor which was due to free π-electrons of conjugated $(\text{-C=N-})_n$ bond.

Generally, on these polymerization reactions of cyano-groups, it is considered that the free energy change ΔG is positive, because the estimated value of ΔH is not less than zero and that of the ΔS is negative. So the high pressure and temperature condition is necessary for the polymerization.

The P-T areas of the polymerization of malononitrile and succinonitrile are shown in Figs. 21 and 22. The area of polymerization is below that of the decomposition. The P-T area of succinonitrile is higher than that of malononitrile. The polymerization yields of malononitrile are dependent on the size of crystal (the finer crystal makes the higher yield). This means that the reaction occurs in

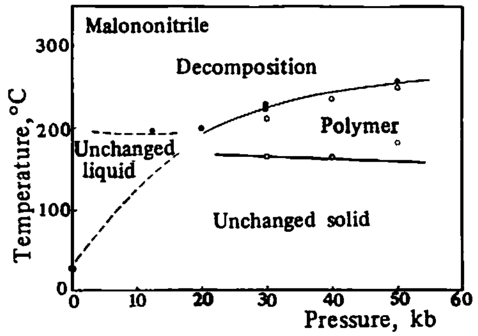

Fig. 21

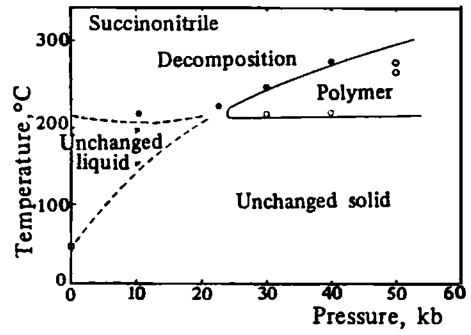

Fig. 22

solid state. But those of succinonitrile are not dependent on the size. This may be due to the glassy solid state of succinonitrile.

The rate of organic solid state reactions at high pressure is difficult to measure, but the rate curves obtained are S-type and have the induction period. The higher the pressure is , the shorter the period is. The activation energy becomes higher by the elevation of pressure. The mechanism of the reaction could be understood according to those of normal conditions. The acceleration by pressure is due to the favorable orientation of monomer to polymerize by the strong dipole interaction of cyano-groups. The polymerization of cyano-groups is chiefly intermolecular in malono- and succinonitriles.

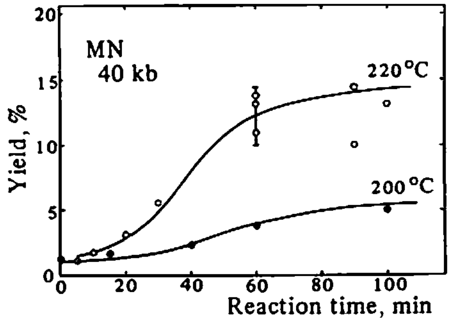

Fig. 23

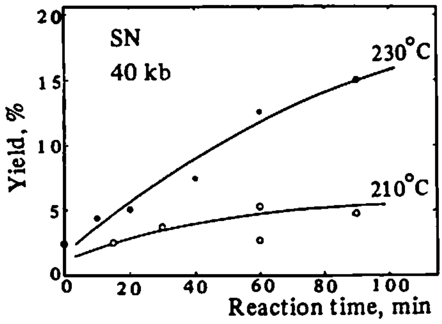

Fig. 24

On the other hand, the polymerization of cyanogroups in polyacrylonitrile is measured by the same method. The rate of the reaction is retarded by pressure. This shows the bulky transition state which is formed by the intramolecular interaction between C≡N group and C–H group.

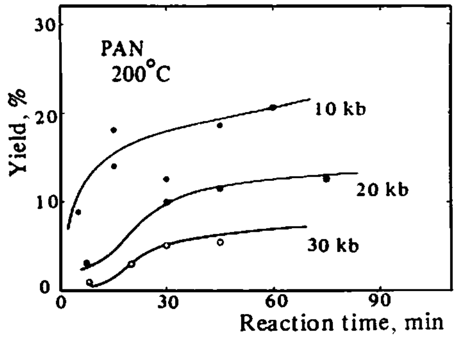

Fig. 25

In addition, I wish to mention on the explosion of organic solid materials. Researchers of very high pressures have experiences on the explosion of organic materials at the instance of pressure release from 30 kb or above to zero, for example, polyester, epoxy-resin, polyamide, polyethylene do explode, (but polytetrafluoroethylene does not explode.)

As I mentioned before, at this pressure range, molecules are deformed and potential among molecules is repulsive. And it may be possible that the potential energy curves cross each other or induce the tunneling effect. Once it happens, some chemical changes occur, and then the explosive chain is initiated and propagates. These may be the reason of explosion. We roughly eatimated the probability of the tunneling effect, which is increased by one thousand times by the 30% decrease of volume (the 11% decrease of intermolecular distance).

Acknowledgments

I wish to express my sincere thanks to Professor K. Monobe and his co-workers in Okayama University, and to Mr. K. Hara in Kyoto University for their collaboration.

Reference

J. Osugi, K. Hara, N. Hirai and J. Hikasa, *This Journal*, **34**, 59 (1964)
J. Osugi and K. Hara, *ibid.*, **36**, 28 (1966)
J. Osugi and T. Mizukami, *Nippon Kagaku Zasshi*, **87**, 1157 (1966)
J. Osugi, K. Hamanoue and N. Otani, *ibid.*, **89**, 532 (1968)
K. Hara, *This Journal*, **40**, 73 (1970)